EXPERIMENTAL VALIDATION AND OPTIMIZATION OF PLC-CONTROLLED HYBRID SOLAR-DIESEL HEATING SYSTEMS IN EXTREME HIGH ALTITUDE CLIMATES

by

Alper CECEN[a]* and Zafer GEMICI[a]

Faculty of Mechanical Engineering, Yildiz Technical University, Istanbul, Turkiye

Original scientific paper
https://doi.org/10.2298/TSCI260330082C

Integrating renewable energy technologies in severe environments presents formidable operational and thermodynamic challenges. This study investigates the performance of a large-scale hybrid solar-diesel heating system for a facility in Van, Turkiye, characterized by an extreme altitude of 2,300 m and a design outdoor temperature of –27 °C. The research quantifies the thermodynamic efficiency gains of transitioning from conventional manual operation to a programmable logic controller (PLC) based automated cascade control regime. A high-fidelity digital twin model was validated against a continuous 20-day spring transition window (April 23-May 13, 2026) using empirical supervisory control and data acquisition temperature logs recorded at 15 minutes intervals. Statistical validation confirmed model reliability with a mean bias error of 7.34% and a coefficient of variation of the root mean square error of 8.26%, strictly adhering to international building energy modeling calibration standards. The automated differential cascade control effectively eliminated human operational errors and inefficient boiler short-cycling. Transitioning to full automation achieved a weather-normalized reduction of 53.7% in monthly diesel fuel consumption and mitigated approximately 5.35 tons of CO_2 equivalent emissions per month. This research establishes a highly reproducible validation framework for hybrid industrial facilities operating under severe environmental and instrumentation constraints.

Keywords: *solar energy, hybrid heating system, energy efficiency, automation control, domestic hot water, extreme cold climate*

Introduction

The building sector accounts for approximately 40% of total global energy consumption, driving a significant portion of worldwide environmental degradation [1]. To mitigate these impacts, transitioning to solar-oriented technologies provides a highly sustainable strategy, particularly in countries characterized by diverse climatic zones such as Turkiye [2, 3]. While the integration of renewable energy is fundamental to long-term decarbonization goals, the operational performance of solar-assisted thermal systems remains highly sensitive to local meteorological variables and the intermittent nature of solar radiation [4, 5]. Consequently, incorporating auxiliary heat sources and implementing multi-generation configurations become mandatory to ensure uninterrupted system reliability and optimal overall efficiency [6, 7].

* Corresponding author, e-mail: alper.cecen@std.yildiz.edu.tr

Recent advancements have also explored modern loop heat pipes to enhance initial heat transfer efficiency within these arrays [8].

Although comprehensive operational baselines for solar thermal systems have been successfully established in sub-tropical and temperate climates [9, 10], deploying these technologies in freezing and extreme high altitude environments introduces severe thermodynamic challenges. Conventional solar thermal arrays frequently suffer from excessive thermal losses, fluid freezing risks, and marked operational inefficiencies in sub-zero ambient conditions [11, 12]. Heat transfer coefficients and module performance metrics under ultra low temperatures deviate significantly from standard operational conditions [13]. Furthermore, specific extreme boundary conditions, such as high altitude combined with low atmospheric pressure, substantially alter the convective and radiative heat loss mechanisms of flat-plate collectors. Convective heat losses decrease significantly with increasing altitude, leading to approximately a 10% variation in the overall heat loss coefficient across different elevations [14]. To maintain thermal stability under such harsh boundary conditions, establishing precise thermal stratification within storage vessels [15] and integrating advanced buffering mechanisms, such as phase-change materials, are highly critical [16, 17].

Managing these complex, highly variable thermal dynamics necessitates the implementation of robust automation and control frameworks. Dynamic control regimes and smart energy management algorithms based on load demand profiles are vital for minimizing excessive auxiliary fuel consumption and optimizing the utilization of solar-driven storage [18-20]. Optimized cascade control allows systems to respond effectively to variable user demands, ensuring compliance with strict building energy codes while yielding measurable economic and environmental benefits [21, 22]. In complex hybrid installations, integrating PLC architectures, often supported by low-cost data acquisition modules and advanced logic algorithms, has emerged as an effective standard for increasing system resilience against extreme climatic fluctuations and minimizing fossil fuel dependency. While advanced strategies like model predictive control (MPC) offer theoretical optimization benefits, PLC-based cascade architectures provide unparalleled robustness, lower computational overhead, and financial feasibility for remote, resource-constrained environments. Prior to physical implementation, dynamic simulation tools like ENERGYPLUS provide critical insights into these multi-variable interactions. However, theoretical models often fail to capture real-world operational deviations, short-cycling phenomena, and field-specific anomalies, making empirical validation mandatory.

An analysis of the existing literature reveals a critical gap regarding the empirical evaluation of transitioning from manual operation to a fully automated PLC cascade control regime in extreme high altitude (2300 m) and sub-zero (–27 °C design temperature) climates. Specifically, operational optimization and empirical efficiency analyses for large-scale hybrid facilities in extreme regions like Baskale (Van, Turkiye) remain largely unaddressed. Unlike conventional configurations optimized for temperate sea-level zones, this study contextualizes the operational challenges under micro-climatic low atmospheric pressure, bridging a specific validation gap highlighted in recent industrial energy management studies. The fundamental novelty of this research lies in its methodological approach to extreme-climate energy management: it provides a field-validated digital twin framework that circumvents the need for expensive inline flowmeters and pyranometers. By relying on high resolution, 15 minutes empirical SCADA temperature logs, ΔT, and precise pump runtime tracking under ASHRAE guidelines, this study establishes a highly reproducible methodology for calibrating digital twins (DESIGNBUILDER/ENERGYPLUS) and optimizing cascade control algorithms in remote, instrumentation-constrained industrial facilities.

Material and method

This study implements an empirical and simulation-based hybrid methodology to evaluate the operational transition from a traditional manual regime to a PLC driven automated cascade architecture. The facility under investigation operates under extreme sub-zero boundary conditions, presenting unique thermodynamic and mechanical challenges.

Figure 1. Layout of system components; (a) the 3-D image of the facility, (b) automation control interface, (c) boiler room, (d) solar collector area, (e) temperature and pressure sensor, (f) automatic solar liquid supply unit, and (g) tanks and circulation pumps

Facility description and extreme boundary conditions

The study site is located in Baskale (Van, Turkiye), situated at an altitude of 2300 m. The region is classified as an *extreme cold climate* with a design outdoor temperature of –27 °C. The facility is a guesthouse with a 150 persons capacity, characterized by an intermittent domestic hot water (DHW) demand profile peaking between 06:00-08:00 and 18:00-21:00. The spatial layout of the system components is illustrated in fig. 1. The central hybrid plant configuration comprises the following interconnected sub-systems:

– *Solar collector array.* The 48 planar flat-plate collectors providing a total gross surface area of 111.84 m². To strictly prevent freeze-induced mechanical failures and thermal locking under extreme sub-zero ambient conditions (down to –40 °C), the primary loop circulates a 60% water-propylene glycol mixture.
– *Auxiliary thermal power.* The auxiliary heating system consists of three cascading diesel-fired hot water boilers, each rated at a nominal thermal output of 581 kW, delivering a combined total installed capacity of 1.74 MW. This massive configuration was historically designed to accommodate legacy institutional redundancy mandates and combined space

heating loads. However, when serving exclusively a 150 persons DHW load, this gross oversizing severely exacerbates the risk of rapid, highly inefficient burner short-cycling under unautomated manual control. This makes an optimized PLC-based cascade management framework critical to regulating burner ignition stages and preventing fuel wastage.

– *Thermal energy storage.* A cumulative storage capacity of 8000 L, divided across four interconnected 2000 L vertical stratified vessels. The tanks are arranged in a series-parallel hydraulic configuration to optimize thermal stratification, maximize solar fraction buffering, and meet instantaneous peak demands.
– *Building envelope boundary.* The overall thermal transmittance (U-values) for the external wall assemblies and roof structure are established at 0.258 W/m²K and 0.267 W/m²K, respectively, providing high thermal resistance to mitigate building envelope transmission losses under sub-zero conditions.
– *Regional climatology.* The historical 30 years baseline of monthly meteorological fluctuations for the Baskale region is summarized in fig. 2.

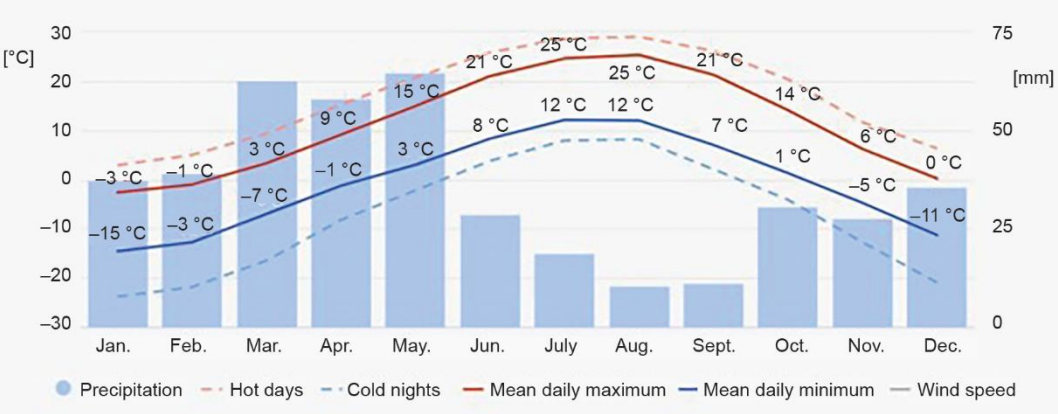

Figure 2. Monthly meteorological values based on Van/Baskale 30 years data [23]

Automation and control logic (PLC)

To maximize renewable energy yield and prevent auxiliary short-cycling, an advanced PLC framework was deployed using differential thermostat logic. Governed by the operational execution flowchart, detailed in fig. 3, the primary solar circulation pump, P_1, is controlled via high resolution differentials, ΔT, measured between the solar array outlet, T_{coll}, and the lower tank temperature, T_{tank_bot}:

$$\text{Solar pump ON: } (T_{coll} - T_{tank_bot}) > 8\ °C$$

$$\text{Solar pump OFF: } (T_{coll} - T_{tank_bot}) < 2\ °C$$

This strict hysteresis loop prevents reverse thermal losses from the storage vessels back to the collector array during periods of low solar irradiance.

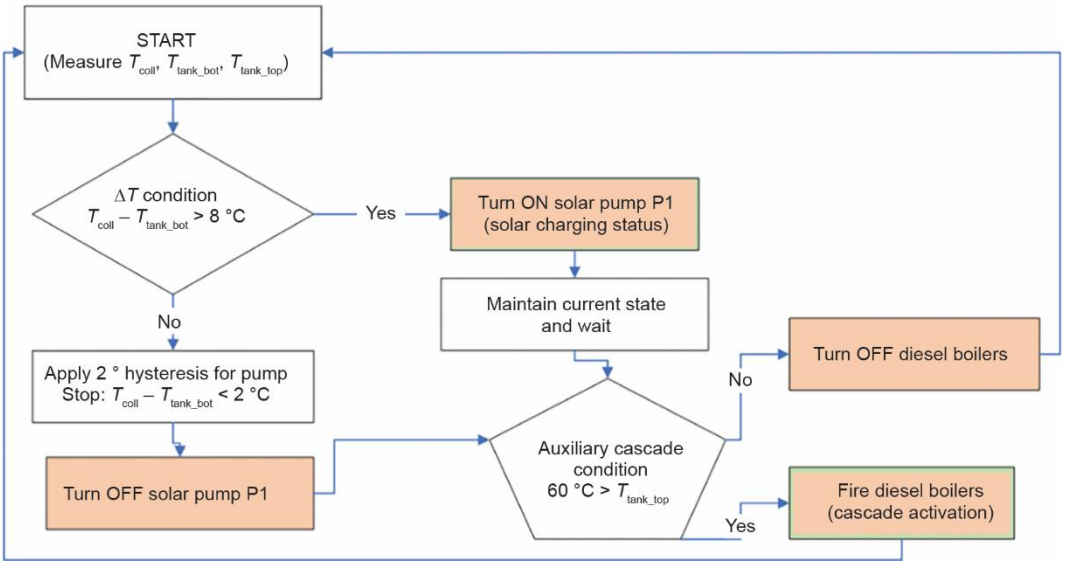

Figure 3. Operational flowchart of the proposed automated PLC control strategy

Auxiliary cascade management, the primary controller dynamically fires the standby diesel burners only when the upper thermal storage node, T_{tank_top}, drops below the critical set-point threshold of 45 °C. This specific high temperature set-point was established to maintain strict DHW hygiene standards against Legionella pneumophila proliferation, while guaranteeing uninterrupted comfort delivery.

Numerical modeling: digital twin development

Due to budgetary and infrastructural constraints inherent to the remote installation site, expensive empirical instruments such as real-time pyranometers and instantaneous inline flowmeters were omitted. To overcome this data limitation, a high-fidelity digital twin was constructed within the DESIGNBUILDER environment (powered by the ENERGYPLUS dynamic simulation engine), fig. 4. Mechanical components and baseline catalog properties were mapped directly to the numerical *Plant Loop* architecture, as outlined in tab. 1.

To rigorously address the equifinality risk arising from the lack of direct solar irradiance sensors, a multi-node thermal balance check was imposed on the storage volume. The boundary errors propagating into the fuel consumption estimations were mathematically bounded through standard differential error propagation metrics.

The actual DHW draw-off mass flow rates and empirical user profiles were successfully reverse-engineered and calibrated by tracking high resolution SCADA pump runtimes alongside thermal decay rates observed across the storage nodes. To resolve identifiability challenges without inline flowmeters, transient thermal energy balance equations) were applied to the storage tank control volumes during periods of pure draw-off (when solar and auxiliary energy inputs were inactive).

Table 1. Digital twin (DESIGNBUILDER) system parameters

System component	Parameter description	Assigned value in digital twin
Flat-plate solar collector array	Collector classification	Planar flat plate
	Total number of collectors	48 units
	Total gross surface area	111.84 m²
	Collector tilt angle/azimuth, β	39° / south
	Baseline optical efficiency	0.76
	Primary heat transfer fluid	60% water-propylene glycol solution
Auxiliary boiler plant	Boiler classification	Diesel-fired hot water boiler
	Unit configuration	3 units (2 duty, 1 standby)
	Nominal thermal capacity	581 kW per unit
	Nominal combustion efficiency	97%
	Automation control strategy	Cascade sequencing operation
Thermal energy storage	Geometric type	Vertical cylindrical, dual serpentine
	Total number of tanks	4 units
	Volumetric capacity per tank	2000 L
	Total system capacity	8000 L
	Hydraulic configuration	Parallel/series stratified
Automation and control system	Controller architecture	PLC-based (AD 598 module)
	Solar loop control logic	Differential temperature, ΔT
	Auxiliary boiler control logic	Upper tank node set-point, 45 °C
	Primary circulation pump power	370 W (nominal electrical input)
	PLC control panel base load	20 W (continuous standby power)

Figure 4. The 2-D floor plan layout and 3-D isometric view of the facility digital twin generated within the DESIGNBUILDER environment

The DESIGNBUILDER software, powered by the ENERGYPLUS dynamic simulation engine, was specifically selected for this study due to its robust heat balance method algorithms and its proven capability to accurately model transient thermal stratification within multi-node storage tanks, fig. 5. Furthermore, its *Detailed HVAC* module allows for the explicit mathematical representation of differential cascade control logics and boiler part-load performance curves, which are strictly required for hybrid plant optimization. Crucially, the simulation engine dynamically recalculates the convective and radiative heat loss coefficients of the flat-plate collectors by implicitly integrating the localized barometric pressure (~77 kPa) and altitude-dependent air density profiles provided within the Meteoblue environmental weather file.

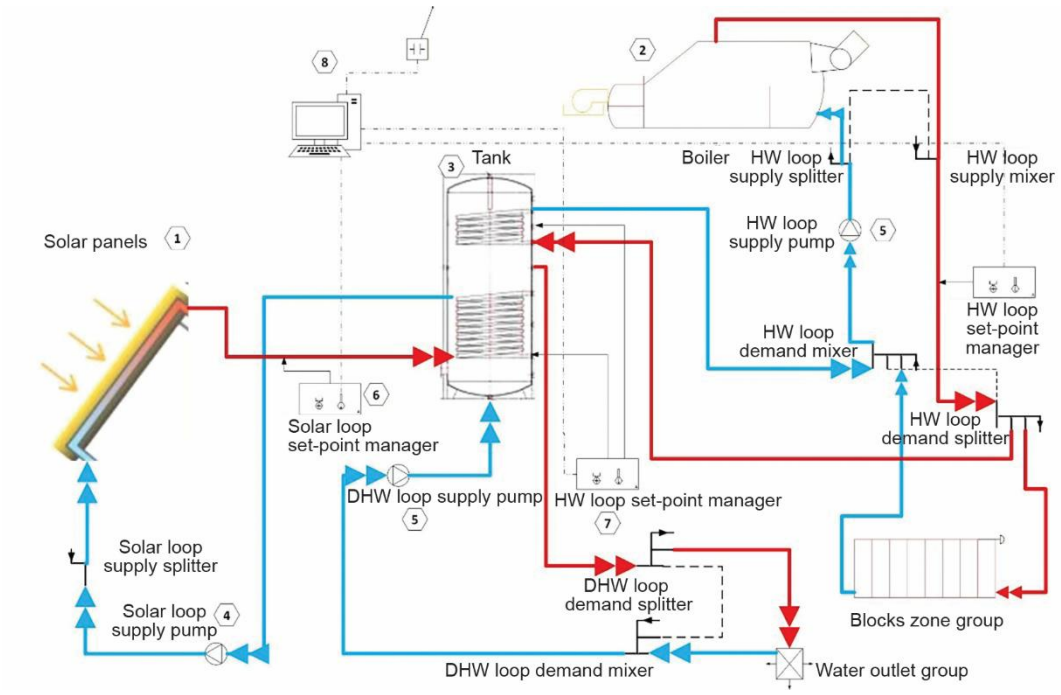

Figure 5. Piping and instrumentation diagram of the hybrid heating plant:
1 – planar flat-plate solar collectors, 2 – 581 kW diesel boilers, 3 – 2.000 L stratified storage tanks, 4 – solar loop pump, 5 – boiler shunt pumps, 6 – solar collector outlet sensor, T_{coll}, 7 – upper/lower tank sensors, T_{tank_top}/T_{tank_bot}, 8 – automation controller, and outdoor ambient thermistor, T_a

Validation and uncertainty analysis

The dynamic fidelity of the established digital twin was verified by overlaying numerical predictions directly against empirical SCADA logs extracted during the 20 days transition period (April 23-May 13, 2026), as demonstrated in fig. 6. While this specific window represents early spring conditions rather than the extreme design winter minimums, it provided a sufficiently high dynamic range of solar irradiance and nocturnal thermal decay to robustly identify the system's transient thermal response and validate the differential control boundaries. The selection of this specific transition window is mathematically deliberate; unlike steady-state winter operational regimes where the auxiliary system runs almost continuously, the

spring transition induces highly volatile, bi-directional thermal fluxes. It captures both sub-zero nocturnal thermal depletion and intense daytime solar fractions within the same diurnal cycles. Consequently, validating the model under these highly transient boundary conditions ensures that the structural thermal mass, multi-node tank stratification, and sensor hysteresis loops are calibrated against the highest possible operational gradient, thereby guaranteeing the model numerical stability and predictive accuracy when extrapolated across the full annualized simulation.

Statistical compliance was evaluated strictly under the criteria established by ASHRAE Guideline 14, employing the mean bias error (MBE) and the coefficient of variation of root mean square error, CV(RMSE):

$$MBE\ (\%) = \frac{\sum_{i=1}^{n}(S_i - M_i)}{\sum_{i=1}^{n} M_i} \cdot 100 \tag{1}$$

$$CV(RMSE)(\%) = \frac{\sqrt{\frac{\sum_{i=1}^{n}(S_i - M_i)^2}{n}}}{\bar{M}} \cdot 100 \tag{2}$$

where S_i is the numerical simulation variable, $\bar{M}$ – the average of the values measured in the field, and M_i – the corresponding empirical measurement recorded on-site. Although ASHRAE Guideline 14 is traditionally applied to whole-building energy consumption, utilizing it for high resolution thermal node temperatures is a well documented and highly reliable proxy approach for component level measurement and verification in instrumentation-constrained setups where direct mass-flow and energy-metering are unavailable. High fidelity calibrated models require an MBE threshold within ±10% and a CV(RMSE) below 30%.

Measurement sensitivity and uncertainty analysis

The spatial distribution of the measurement nodes was strategically established to capture the critical boundary conditions of the plant loop. The PT1000 immersion-type sensors were installed directly within thermowells at the collector array outlet, T_{coll}, and at specific vertical nodes within the primary storage tanks to monitor thermal stratification. Signal transmission to the main PLC architecture was facilitated via hardwired connections, ensuring high data transmission reliability and eliminating the signal latency or packet-loss issues common in wireless setups. Systemic error sources, including the thermal inertia of the thermowells, were mitigated by applying moving-average filtering protocols during the post-processing of the 15 minutes SCADA logs.

Adhering to the methodological frameworks validated in recent literature for constrained field setups, overall performance uncertainty was derived strictly from localized temperature differentials. The physical sensitivities and baseline precision limits of the deployed SCADA sensor architecture are detailed in tab 2.

Table 2. Characteristics and sensitivities of field measuring devices

Measurement parameter	Sensor type	Measurement range	Precision
Collector outlet temperature, T_{coll}	PT1000 immersion type	–50 °C ~ +200 °C	±0.3 °C
Lower tank temperature, T_{tank_bot}	PT1000 immersion type	–50 °C ~ +200 °C	±0.3 °C
Outside air temperature, T_a	NTC thermistor	–40 °C ~ +80 °C	±0.5 °C
Datalogging	PLC SCADA module	Every 15 minutes	±0.1%

Cumulative experimental uncertainty, $W_{\Delta T}$, governing the primary control variable, $\Delta T = T_{coll} - T_{tank_bot}$, was computed *via* the standard root sum square propagation method:

$$W_{\Delta T} = \sqrt{(w_{T_{coll}})^2 + (w_{T_{tank_bot}})^2} \tag{3}$$

Applying the sensor precision values, w_i = 0.3 °C, from tab. 2, the equation yields a maximum cumulative uncertainty of ±0.42 °C. This low margin of empirical error confirms that the differential control loop operates reliably without encountering false triggers at the 8 °C activation or 2 °C deactivation boundaries.

Results and discussion

Validation of the simulation model and thermal stability

The dynamic fidelity of the established digital twin was verified by overlaying numerical predictions directly against continuous empirical SCADA logs extracted during the extended 20 days spring transition period (April 23-May 13, 2026), as demonstrated in fig. 6. Statistical evaluation of this baseline calibration yielded an overall MBE of 7.34% and a CV(RMSE) of 8.26%. Both metrics strictly comply with the validation thresholds defined by ASHRAE Guideline 14, which mandates an $MBE \leq \pm 10\%$ and a $CV(RMSE) \leq \pm 30\%$ for hourly and sub-hourly energy model calibrations.

To contextualize these calibration boundaries, the achieved statistical accuracy shows a superior or equivalent alignment compared to recent multi-generation digital twin studies. Specifically, the observed CV(RMSE) of 8.26% outperforms the solar-assisted heating models developed by Figaj and Zoladek [24], which noted alignment deviations hovering around 11.4% due to uncontrolled macro-climatic fluctuations. Furthermore, our temperature-only calibration methodology yields a precision level that closely matches the single-stage ideal load calibration frameworks optimized by Guerrero Ramirez *et al.* [25]. This proves that indirect sensor tracking through high resolution temperature differentials, ΔT, can robustly substitute for direct online flow-metering and on-site solar radiation instrumentation in instrumentation-constrained industrial applications.

Thermodynamically, the empirical data confirmed the effectiveness of the automated control regime under extreme boundary conditions. Governed by the differential logic loop, primary glycol circulation initiated precisely at optimal thermal collection thresholds, entirely eliminating freeze risks and severe convective heat losses common during extreme sub-zero morning hours. Furthermore, severe thermal draw-offs triggered by the 150 persons peak DHW demand were effectively mitigated.

In the historical manual regime, sudden drops in upper tank temperatures caused operators to manually fire the auxiliary boilers, resulting in severe short-cycling exacerbated by

the massive 1.74 MW installed capacity. Conversely, the automated PLC cascade logic successfully buffered these peaks by utilizing stratified thermal storage, delaying fossil-fuel ignition until the renewable thermal potential was completely exhausted.

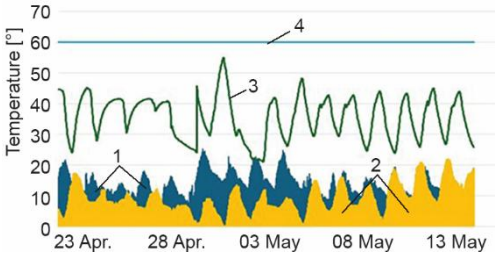

Figure 6. Verification of simulation boiler temperatures with real SCADA data taken on 23 April-13 May, 2026*;*
1 – SCADA outside air temperature (from the field), 2 – DESIGNBUILDER outside dry-bulb temperature, 3 – SCADA real tank – Mi, and 4 – ideal tank temperature

Energy savings and fuel consumption reduction

Empirical baseline data for the unautomated manual regime, *Scenario 1*, was aggregated from facility logbooks recorded during the severe winter conditions of March 2026. Due to human operational delays and extreme ambient temperatures dropping to –27 °C, the auxiliary diesel burners operated with frequent, highly inefficient short-cycles to counter rapid thermal losses. Historical records confirm that manual operation consumed an average of 120 L of diesel fuel daily, totaling 3720 L for the month.

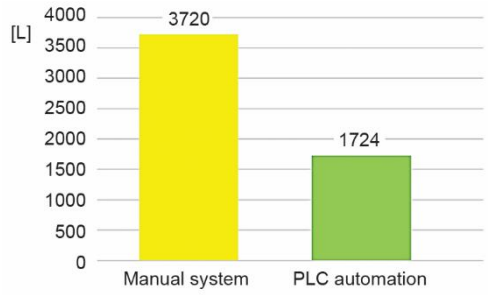

Figure 7. Comparison of monthly diesel fuel consumption of the existing manual system and PLC automation system

To evaluate the automated framework, *Scenario 2*, the calibrated digital twin was subjected to the identical historical micro-climate weather file and empirical DHW draw-off profiles from the baseline period. Numerical simulations confirmed that transitioning to full PLC automation reduced monthly diesel consumption to 1724 L, achieving a projected net fossil fuel reduction of 53.7%, fig. 7. This operational shift is estimated to mitigate local atmospheric emissions by approximately 5.35 tons of CO_2 equivalent per month.

To rigorously validate these thermodynamic efficiency gains, the absolute net primary energy savings, ΔE_{net}, were formulated by accounting for the continuous parasitic electrical consumption of the automation modules, sensors, and circulation pumps:

$$\Delta E_{\text{net}} = \Delta Q_{\text{thermal}} - \sum_{i=1}^{n} (E_{\text{elec},i}\lambda) \tag{4}$$

where $\Delta Q_{\text{thermal}}$ [kWh] is the gross thermal energy saved from diesel fuel reduction, $E_{\text{elec},i}$ [kWh] – the electrical energy consumed by the i^{th} automation and pumping component, and λ [–] – the primary energy conversion factor for regional electricity.

As illustrated in fig. 6, this massive primary energy reduction was achieved while simultaneously maintaining strict thermal set-points (60 °C). The underlying mechanism driving this efficiency gain is heavily attributed to eliminating severe human-induced operational errors, such as leaving boilers running idly during low demand periods and entirely wasting the

available solar potential. To address whether simpler, baseline rule-based modifications (such as basic anti-short-cycling timers or manual stage-delay switches) could yield equivalent performance, it is critical to highlight that the proposed PLC framework operates as an integrated multi-variable cascade. Traditional unautomated or single-variable timer overrides cannot dynamically decouple the massive 1.74 MW boiler plant capacity from the instantaneous multi-node thermal stratification of the 8000 L storage tanks under volatile ambient temperatures dropping to –27 °C. By dynamically binding the auxiliary cascade trigger exclusively to the upper tank node, $T_{\text{tank,top}}$, while running the solar collection loop on a strict 8 °C/2 °C hysteresis, the proposed controller achieves a tight thermodynamic boundary control that a decoupled or static rule-based system cannot maintain without either risking fluid freezing or inducing premature burner ignition.

Economic analysis and payback period

Beyond thermodynamic optimization, the transition to a PLC-based automated cascade regime yields highly favorable economic outcomes. The initial capital expenditure for implementing the automation infrastructure, including the central PLC modules, digital differential thermostats, sensor networks, electrical panel revisions, and integration labor, is estimated at approximately €4500.

Conversely, the empirical and simulated data confirms a net operational saving of nearly 2000 L of diesel fuel during extreme winter months. Given the elevated logistical and transportation costs of fossil fuel delivery to remote high altitude regions, this fuel reduction translates to direct and substantial financial savings. Based on regional fuel price baselines (approximately €1.28 per L, based on Energy Market Regulatory Authority data), the calculation integrates seasonal fluctuations over a full 12 months heating period. While peak winter savings reach nearly €2560 per month, spring and summer savings are considerably lower due to naturally high solar fractions. Accounting for this seasonal variation, the annualized simple payback period for this automation investment is calculated to be well within a single heating season (approximately 8-10 months). This exceptional cost-effectiveness demonstrates that intelligent cascade automation is not merely a technical necessity for thermal stability, but a highly feasible and high return financial strategy for remote hybrid heating facilities.

Conclusions

This study evaluated the operational performance and automation-driven efficiency gains of a large-scale hybrid solar-diesel heating system operating under extreme climatic conditions (2300 m altitude, –27 °C design temperature). The primary findings are summarized as follows:

- *Methodological framework.* Despite severe on-site instrumentation constraints (absence of pyranometers and flowmeters), a high-fidelity digital twin was successfully established. Validated against 15 minutes SCADA temperature logs, the model achieved an MBE of 7.34% and a CV(RMSE) of 8.26%, demonstrating that reliable energy performance baselines can be established through temperature-based digital twin calibration in remote facilities.
- *Operational efficiency.* The transition from manual operation to a PLC-driven automation regime successfully eliminated auxiliary boiler short-cycling and human-induced operational errors. Crucially, the automation buffered the rapid cycling tendencies caused by the historical 1.74 MW gross oversizing of the auxiliary boiler plant. The differential temperature control (solar pump ON at $\Delta T > 8$ °C, OFF at $\Delta T < 2$ °C) ensured maximum solar

energy utilization while safeguarding the system against freezing risks during extreme subzero morning hours.

- *Fossil fuel reduction.* By comparing the weather-normalized numerical baseline of the automated system against the historical manual operation logs for the identical period, the implementation of an automated cascade management strategy yielded a net reduction of 53.7% in monthly diesel fuel consumption compared to the manual operational baseline. This confirms that automation is the most critical factor in mitigating fossil fuel dependency in hybrid installations.
- *Environmental impact.* The optimized energy management regime resulted in a monthly atmospheric emission reduction of approximately 5.35 tons of CO_2 equivalent, significantly enhancing the environmental sustainability of the facility.
- *Thermodynamic contribution.* The study provides a validated baseline for the design of hybrid systems in extreme geographies, empirically supporting the necessity of automated energy management to overcome the thermodynamic challenges of low atmospheric pressure and high altitude thermal losses.
- The major operational limitation of this framework lies in the lack of direct local solar pyranometers, which necessitates indirect temperature-based tracking. Furthermore, practical implementation in such extreme environments presents unique logistical challenges.

The handling of high-concentration (60%) glycol mixtures at temperatures dropping down to –27 °C requires specialized automated feed units to prevent pump cavitation, while the risk of sensor freezing demands robust weatherproofing for all external SCADA communication lines. Future design projects must account for these harsh installation constraints alongside thermodynamic parameters.

Future research directions will focus on the integration of MPC algorithms to explicitly handle peak load uncertainties and the incorporation of PCM into the storage network to further enhance thermal stability and the renewable energy fraction in extreme climates.

Acknowledgment

The authors would like to express their sincere gratitude to Prof. Dr. Zafer GEMICI for his valuable guidance and academic contributions throughout the planning and execution of this study. We are also grateful to the site personnel in Baskale for their technical support during field studies and to the relevant authorities for their contributions to data collection.

Nomenclature

M_i – empirically measured field value, [–]
$\bar{M}$ – mean of the empirically measured values, [–]
n – total number of data samples or time steps, [–]
Q – heat transfer rate or thermal power, [kW]
S_i – simulation output value, [–]
T – temperature, [°C]
w_i – absolute precision/uncertainty of sensor i, [°C]
$W_{\Delta T}$ – cumulative experimental uncertainty of differential temperature, [°C]

Greek symbols

Δ – difference or finite change
λ – primary energy conversion factor for regional electricity

Acronyms

CV(RMSE) – coefficient of variation of root mean square error
DHW – domestic hot water
HW – hot water
MBE – mean bias error
MPC – model predictive control
PLC – programmable logic controller
SCADA – supervisory control and data acquisition

References

[1] Azaza, M., *et al*., A Study on the Viability of an On-Site Combined Heat – and Power Supply System with and Without Electricity Storage for Office Building, *Energy Conversion and Management, 213* (2020), 112807
[2] Uctug, F. G., Azapagic, A., Life Cycle Environmental Impacts of Domestic Solar Water Heaters in Turkey: The Effect of Different Climatic Regions, *Science of The Total Environment, 622.623* (2018), May, pp. 1202-1216
[3] Madhuri, R. V. S., *et al*., Solar Energy-Driven Desalination: A Renewable Solution for Climate Change Mitigation and Advancing Sustainable Development Goals, *Desalination, 602* (2025), 118575
[4] Emami, A. M., *et al*., Exergy-Economic Based Multi-Objective Optimization and Carbon Footprint Analysis of Solar Thermal Refrigeration Systems, *Case Studies in Thermal Engineering, 64* (2024), 105425
[5] Bicer, Y., Dincer, I., Analysis and Performance Evaluation of a Renewable Energy Based Multigeneration System, *Energy, 94* (2016), Jan., pp. 623-632
[6] Al-Smairan, M., *et al*., Techno-Economic Investigation of an Integrated Boiler-Solar Water Heating/Cooling System: A Case Study, *Energies, 14* (2021), 1, 1
[7] Zhang, D., *et al*., Numerical Study on Solar Heating System with Different Auxiliary Heat Sources, *Thermal Science and Engineering Progress, 54* (2024), 102845
[8] Singh, A. K., Kumar, R., Enhancing Renewable Energy Systems Using Loop Heat Pipes: A Case Research on Solar Thermal Applications, *Applied Thermal Engineering, 275* (2025), 126866
[9] Chow, T. T., *et al*., Modeling and Application of Direct-Expansion Solar-Assisted Heat Pump for Water Heating in Subtropical Hong Kong, *Applied Energy, 87* (2010), 2, pp. 643-649
[10] Arsalan, M., *et al*., Experimental Development, Techno-Economic and Environmental Analysis of a Hybrid Solar Space Heating System in a Subtropical Climate, *Energy Reports, 10* (2023), Nov., pp. 3020-3034
[11] Sokhansefat, T., *et al*., Thermoeconomic and Environmental Analysis of Solar Flat Plate and Evacuated Tube Collectors in Cold Climatic Conditions, *Renewable Energy, 115* (2018), Jan., pp. 501-508
[12] Hachchadi, O., *et al*., Techno-Economic Assessment and Environmental Impact of Photovoltaic and Conventional Solar Water Heating Systems in Cold Climates, *Energy Conversion and Management, 297* (2023), 117725
[13] Dong, G., *et al*., Study on Heat Transfer Performance of Ultra-Low Temperature Radiant Heating Modules, *Thermal Science, 30* (2026), 3B, pp. 2367-2378
[14] Wang, D., *et al*., Comparative Analysis of Heat Loss Performance of Flat Plate Solar Collectors at Different Altitudes, *Solar Energy, 244* (2022), Sept., pp. 490-506
[15] Chandra, Y. P., Matuska, T., Stratification Analysis of Domestic Hot Water Storage Tanks: A Comprehensive Review, *Energy and Buildings, 187* (2019), Mar., pp. 110-131
[16] Abdelsalam, M. Y., *et al*., Hybrid Thermal Energy Storage with Phase Change Materials for Solar Domestic Hot Water Applications: Direct versus Indirect Heat Exchange Systems, *Renewable Energy, 147* (2020), Part 1, pp. 77-88
[17] Tilioua, A., *et al*., Energy Assessment of a Compact Solar Wall-Heating System Powered by a Parabolic Collector, *Next Energy, 9* (2025), 100442
[18] Sonnekalb, T., Lucia, S., Smart Hot Water Control with Learned Human Behavior for Minimal Energy Consumption, *Proceedings* the IEEE 5th World Forum on Internet of Things (WF-IoT), Limerick, Ireland, 2019, pp. 572-577.
[19] Chen, R., *et al*., A New Dynamic Control Strategy for a Solar-Driven Absorption Thermal Energy Storage System: Modeling and Performance Evaluation, *Applied Thermal Engineering, 260* (2025), 124983
[20] Hohne, P. A., *et al*., Optimal Energy Management and Economic Analysis of a Grid-Connected Hybrid Solar Water Heating System: A case of Bloemfontein, South Africa, *Sustainable Energy Technologies and Assessments, 31* (2019), Feb., pp. 273-291
[21] Scolan, S., *et al*., Dynamic Optimization of the Operation of a Solar Thermal Plant, *Solar Energy, 198* (2020), Mar., pp. 643-657
[22] Belmonte, J. F., *et al*., A Stochastic Thermo-Economic Analysis of Solar Domestic Hot-Water Systems in Compliance with Building Energy Code Requirements: The Case of Spain, *Sustainable Energy Technologies and Assessments, 52* (2022), 102007

[23] ***, Meteoblue AG, Simulated Historical Climate & Weather Data for Baskale – Republic of Turkey, https://www.meteoblue.com/
[24] Figaj, R., Zoladek, M., Experimental and Numerical Analysis of Hybrid Solar Heating and Cooling System for a Residential User, *Renewable Energy, 172* (2021), July, pp. 955-967
[25] Guerrero Ramírez, K., *et al*., Single-Stage Calibration of Building Energy Models: Overcoming Data Limitations for Energy Performance Contracts Using an Ideal Loads Air System, *Buildings, 15* (2025), 2, pp. 1-18

Paper submitted: March 30, 2026
Paper revised: May 15, 2026
Paper accepted: May 25, 2026

2026 Published by the Vinča Institute of Nuclear Sciences, Belgrade, Serbia.
This is an open access article distributed under the CC BY 4.0 terms and conditions